Cell Research (2015) 25:335-350.

www.nature.com/cr

ORIGINAL ARTICLE

LncRNA *Dum* interacts with Dnmts to regulate *Dppa2* expression during myogenic differentiation and muscle regeneration

Lijun Wang[1], Yu Zhao[2], Xichen Bao[3], Xihua Zhu[3], Yvonne Ka-yin Kwok[2], Kun Sun[4], Xiaona Chen[2], Yongheng Huang[5], Ralf Jauch[5], Miguel A Esteban[3], Hao Sun[4], Huating Wang[1]

[1]Department of Orthopaedics and Traumatology, Li Ka Shing Institute of Health Sciences, The Chinese University of Hong Kong, Hong Kong, China; [2]Department of Obstetrics and Gynaecology, Li Ka Shing Institute of Health Sciences, The Chinese University of Hong Kong, Hong Kong, China; [3]Laboratory of Chromatin and Human Disease, Key Laboratory of Regenerative Biology, South China Institute for Stem Cell Biology and Regenerative Medicine, Guangzhou Institutes of Biomedicine and Health, Chinese Academy of Sciences, Guangzhou, China; [4]Department of Chemical Pathology, Li Ka Shing Institute of Health Sciences, The Chinese University of Hong Kong, Hong Kong, China; [5]Genome Regulation Laboratory, Guangzhou Institutes of Biomedicine and Health, Chinese Academy of Sciences, Guangzhou, China

Emerging studies document the roles of long non-coding RNAs (LncRNAs) in regulating gene expression at chromatin level but relatively less is known how they regulate DNA methylation. Here we identify an lncRNA, *Dum* (developmental pluripotency-associated 2 (*Dppa2*) Upstream binding Muscle lncRNA) in skeletal myoblast cells. The expression of *Dum* is dynamically regulated during myogenesis *in vitro* and *in vivo*. It is also transcriptionally induced by MyoD binding upon myoblast differentiation. Functional analyses show that it promotes myoblast differentiation and damage-induced muscle regeneration. Mechanistically, *Dum* was found to silence its neighboring gene, *Dppa2*, *in cis* through recruiting Dnmt1, Dnmt3a and Dnmt3b. Furthermore, intrachromosomal looping between *Dum* locus and *Dppa2* promoter is necessary for *Dum/Dppa2* interaction. Collectively, we have identified a novel lncRNA that interacts with Dnmts to regulate myogenesis.

***Keywords*:** LncRNA; *Dum*; myogenesis; *Dppa2*; DNA methylation

Cell Research (2015) **25**:335-350. doi:10.1038/cr.2015.21; published online 17 February 2015

Introduction

Although only a small number of functional long non-coding RNAs (lncRNAs) have been well characterized to date, they seem to control major biological processes impacting cell differentiation and development [1]. Specifically, recent work suggested that a large number of lncRNAs function to epigenetically modulate gene expression through interacting with chromatin modifiers or remodelers. They may act as signals, guides or scaffolds to the chromatin to regulate expression of target genes [2-4]. In some cases, the lncRNA and the target genes are transcribed from the same locus or in a very close distance. In other cases, however, an lncRNA could act over a long distance on a distal target gene. This may involve three-dimensional folding of chromatin which brings the target locus and the lncRNA in a close proximity.

The genesis of skeletal muscle during embryonic development and postnatal life serves as a paradigm for stem and progenitor cell maintenance, lineage specification and terminal differentiation. During injury-induced regeneration, muscle stem cells (satellite cells) are activated, proliferate, differentiate and fuse to form myofibers to repair the damage [5]. The process of myoblast differentiation is a powerful system for investigating the biological functions of lncRNAs because of the availability of an *in vitro* C2C12 murine myoblast cell

Correspondence: Huating Wang[a], Hao Sun[b]
[a]Tel: +(852) 3763-6047; Fax: +(852) 2636-0008
E-mail: huating.wang@cuhk.edu.hk
[b]E-mail: haosun@cuhk.edu.hk
Received 27 May 2014; revised 1 November 2014; accepted 18 November 2014; published online 17 February 2015

line; it can faithfully recapitulate the myogenesis in culture and the transcriptional networks coordinating gene expressions are extensively studied using this cell line. Specification and differentiation of skeletal muscle stem cells (myoblasts) into myotubes are driven by a family of muscle-restricted basic Helix-Loop-Helix transcription factors (TFs), MyoD, Myf5, myogenin and MRF4, which activate the differentiation program by inducing the transcription of muscle-specific genes such as myosin heavy chain (MyHC), alpha actin (α-actin) and troponin isoforms. It is becoming increasingly clear that a complex network of transcription factors, epigenetic regulators and non-coding RNAs is pivotal for myogenesis [6]. The establishment and maintenance of DNA methylation patterns resulting in modulation of gene expression is one of the key steps in epigenetic regulation during muscle cell differentiation. This modification is mediated by the members of the DNA methyltransferase (DNMT) family, conventionally classified as *de novo* (DNMT3a and DNMT3b) and maintenance (DNMT1) Dnmts. DNA methylation is thought to repress many muscle gene loci. For example, it has been shown that DNA methylation helps to restrict myogenin activation and demethylation of myogenin promoter appears necessary for the differentiation program to proceed [7]. However, the precise mechanisms regulating methylation/demethylation in myogenesis is still far from being understood and it remains unclear whether such events are general or specific to a subset of genes. More importantly, although much has been done on how lncRNAs modulate chromatins, very little is known in terms of how they are involved in DNA methylation. The best characterized example is Kcnq1ot1 lncRNA which was shown to interact with DNMT1 to maintain methylation of ubiquitously imprinted genes both in developmental stages and somatic tissues [8]. Very recently, Ruscio AD *et al*. [9] also reported the interaction between DNMT1 and a novel lncRNA, *ecCEBPA*, which interestingly leads to DNMT1 sequestration and prevents *CEBPA* gene locus methylation. However, it is unknown whether other DNMT enzymes (DNMT3a, DNMT3b) may also interact with lncRNAs, through which the patterns of *de novo* DNA methylation can be modulated.

In this study, we identified an lncRNA named *Dum* (developmental pluripotency-associated 2 (*Dppa2*) Upstream binding Muscle lncRNA) in myoblast cells from the *de novo* assembly of high-throughput RNA-sequencing data. The expression of *Dum* is tightly associated with *in vitro* and *in vivo* myogenesis processes and induced by MyoD upon myoblast differentiation. Functional studies demonstrated that it acts as a pro-myogenic factor in both myoblast differentiation and muscle regeneration *in vivo*. Further mechanistic investigation revealed that *Dum* functions by *in cis* silencing of its neighboring gene *Dppa2* through interacting and recruiting multiple Dnmts (Dnmt1, Dnmt3a and Dnmt3b) to its promoter regions; and intrachromosomal looping is necessary for *Dum*/*Dppa2* interaction. Altogether, our studies have uncovered a novel functional lncRNA that modulates DNA methylation.

Results

A lncRNA Dum is associated with skeletal myogenesis

In an attempt to discover the functional lncRNAs associated with myogenesis, we applied an *ab initio* identification pipeline [10] to the RNA-seq data from differentiating C2C12 mouse myoblast cells. Among all the identified lncRNAs, *Dum* is a known transcript transcribed from mouse chromosome 16. An evident Pol II peak that marked its promoter region and an H3K4me3-H3K36me3 domain which typically defines lincRNA locus [11] was also identified. It is annotated in UCSC with three isoforms and in Refseq as 5330426P16Rik (Figure 1A). Through rapid amplification of cDNA ends we demonstrated that 5330426P16Rik is abundantly expressed in C2C12 cells. It contains two exons with a full length of 1 817 bp (Figure 1B and Supplementary information, Figure S1A) as confirmed by northern blotting analysis (Figure 1C and Supplementary information, Figure S1B) and RT-PCR amplification (Figure 1D). A *Dppa2* gene is located in its distant upstream region and transcribes from the opposite strand (Figure 1B). *Dppa2* is highly expressed in pluripotent stem cells and involved in the maintenance of pluripotency of embryonic stem (ES) cells [12]. By RNA-fluorescence *in situ* hybridization (RNA-FISH), *Dum* was found to be distributed in both nucleus and cytoplasm of C2C12 myoblasts, distinct from the nuclear transcript U1 which was mainly found in the nucleus (Figure 1E and Supplementary information, Figure S1C). Consistently, by cellular fractionation assay, almost equal amounts of *Dum* transcripts were found in nuclear and cytoplasmic extracts (Figure 1F); well-known lncRNAs, *Xist*, *Malat1* and *U1*, on the other hand, were mainly detected in the nuclei; and *Yam-1*, as we recently showed [13], was found in both fractions with almost equal amounts. Using our recently developed coding potential predication software iSeeRNA [14], *Dum* is predicated to be a non-coding RNA (data not shown) which folds into extensive stem-loop structures (Supplementary information, Figure S1D). Results from *in vitro* translation assay also confirmed its non-coding nature (Supplementary information, Figure S1E). Interestingly, a human ortholog was predicted on chromosome 3; evi-

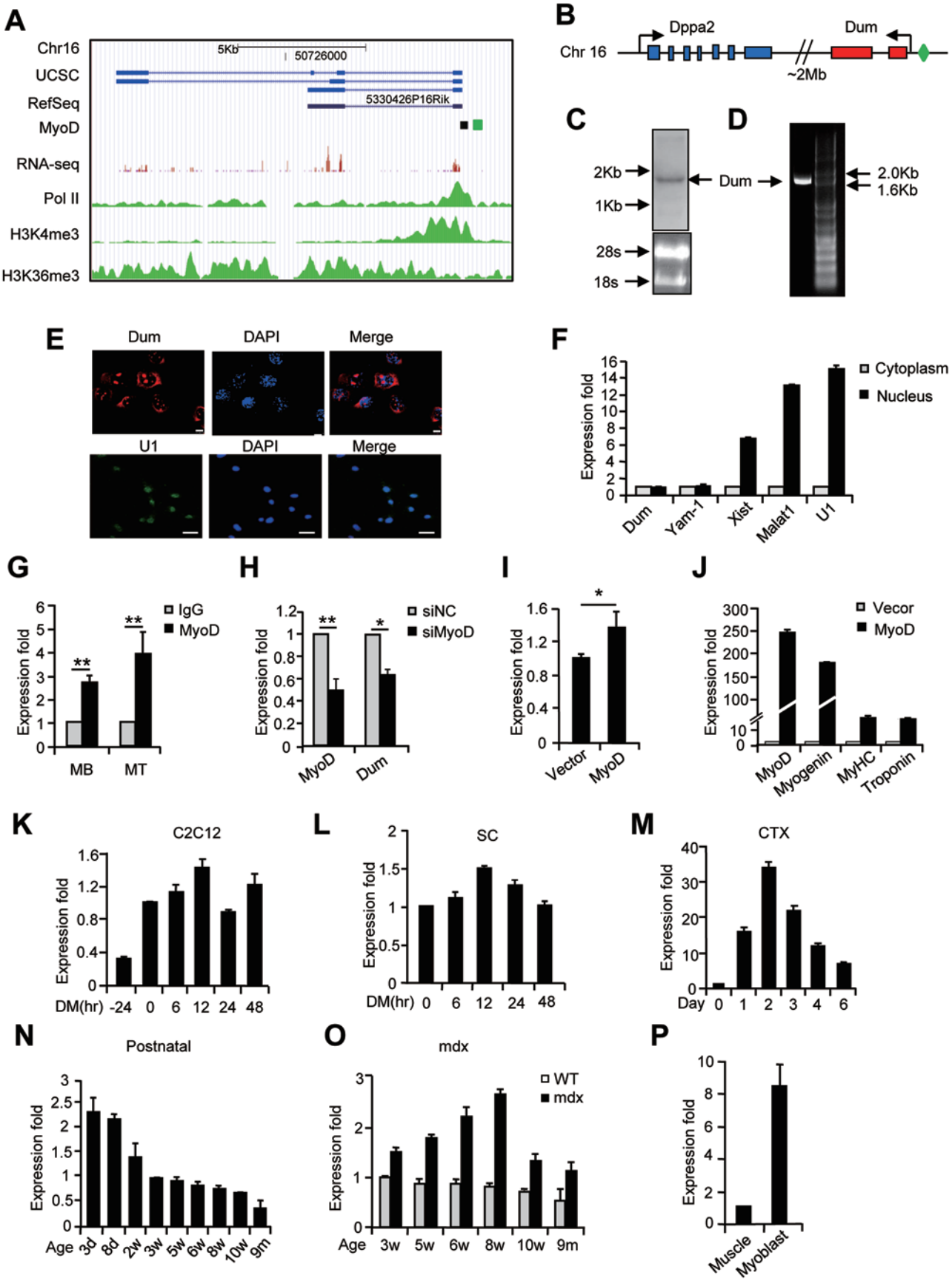
A
Chr16
UCSC
RefSeq
MyoD
RNA-seq
Pol II
H3K4me3
H3K36me3
5Kb
50726000
5330426P16Rik
B
Chr 16
Dppa2
Dum
~2Mb
C
2Kb
1Kb
28s
18s
D
Dum
2.0Kb
1.6Kb
E
Dum
DAPI
Merge
U1
DAPI
Merge
F
Expression fold
Cytoplasm
Nucleus
Dum
Yam-1
Xist
Malat1
U1
G
Expression fold
IgG
MyoD
MB
MT
H
Expression fold
siNC
siMyoD
MyoD
Dum
I
Expression fold
Vector
MyoD
J
Expression fold
Vecor
MyoD
MyoD
Myogenin
MyHC
Troponin
K
C2C12
Expression fold
DM(hr) -24 0 6 12 24 48
L
SC
Expression fold
DM(hr) 0 6 12 24 48
M
CTX
Expression fold
Day 0 1 2 3 4 6
N
Postnatal
Expression fold
Age 3d 8d 2w 3w 5w 6w 8w 10w 9m
O
mdx
Expression fold
WT
mdx
Age 3w 5w 6w 8w 10w 9m
P
Expression fold
Muscle
Myoblast

Figure 1 *Dum* is a novel lncRNA associated with skeletal myogenesis. **(A)** Genomic snapshot of mouse *Dum* generated in UCSC (blue), Refseq (black), MyoD ChIP-seq (green), RNA-seq (pink), Pol II, H3K4me3 and H3K36me3 ChIP-seq (green) tracks. **(B)** Schematic illustration of the genomic location and structure of mouse *Dum* locus. A MyoD-binding site is shown as green diamond. **(C**, **D)** Detection of full-length *Dum* by northern blotting **(C)** or RT-PCR **(D)** in C2C12 myoblasts. **(E)** Visualization of *Dum* or U1 in C2C12 myoblasts by RNA-FISH. Scale bar, 50 μm. **(F)** The expression of *Dum*, *Yam-1*, *Xist*, *Malat1* and *U1* in nuclear or cytoplasmic fraction of C2C12 myoblasts. **(G)** The binding of MyoD on the *Dum* promoter as shown by ChIP-PCR. **(H)** Knockdown of MyoD by siRNA oligos decreased *Dum*. **(I)** Overexpression of a MyoD plasmid in 10T1/2 cells increased *Dum* expression as shown. **(J)** The levels of *MyoD*, *myogenin*, *MyHC* and *troponin* mRNAs were increased in cells from **I**. **(K-P)** The expression of *Dum* was detected by qRT-PCR. The expression of *Dum* in differentiating C2C12 **(K)**; in differentiating satellite cells freshly isolated from mouse limb muscles **(L)**; during CTX-induced regeneration **(M)**; in muscles of postnatal mice at the indicated ages **(N)**; in muscles from wild-type or dystrophic mdx mice at the indicated ages **(O)**; and in mature mouse skeletal muscle tissue or isolated primary myoblasts **(P)**. All PCR data were normalized to *GAPDH* mRNA and represent mean ± SD of three independent experiments. $*P < 0.05$, $**P < 0.01$. See also Supplementary information, Figure S1.

dence of its expression was found in various tissues and cells through exploring GENCODE data (Supplementary information, Figure S1F).

To investigate its relevancy in myogenesis, we first examined whether it is regulated by MyoD, reasoning that a functional lncRNA may be under regulation of the master myogenic transcription factor. By analyzing publically available MyoD ChIP-seq data from C2C12 cells [15], a potential binding peak was identified –26 bp upstream of transcriptional start site (Figure 1A and 1B). Results from ChIP-PCR assay further confirmed the MyoD binding not only in proliferating myoblasts (MBs) but also in differentiating myotubes (MTs) (Figure 1G and Supplementary information, Figure S1G). Consistently, knockdown of MyoD with an siRNA oligo in C2C12 cells significantly decreased *Dum* expression by 35% as compared to negative control (siNC) (Figure 1H); overexpression of a MyoD plasmid in 10T1/2 fibroblast cells, on the other hand, upregulated *Dum* expression (Figure 1I) along with the expression of several myogenic genes *myogenin*, *MyHC* and *troponin* (Figure 1J).

The regulation of *Dum* by MyoD suggested that it is likely a functional lncRNA in skeletal muscle cells. To gain more insights, we first examined its temporal and spatial expression patterns in several myogenesis systems *in vitro* and *in vivo*. During C2C12 cell differentiation, *Dum* was found to be robustly upregulated during the early stage from proliferating myoblasts (–24 h) to 12 h in differentiation medium (DM) but gradually decreased afterwards (24 and 48 h) (Figure 1K), suggesting that it can be a pro-myogenic factor during the early differentiation. Consistently, during the differentiation of freshly isolated satellite cells (SCs), *Dum* expression significantly increased in the early stage (Figure 1L). To further examine its expression dynamics during myogenesis *in vivo*, we employed a widely-used muscle regeneration model in which the intramuscular injection of cardiotoxin (CTX) results in muscle injury and in turn induces muscle regeneration [16]. *Dum* was found to be highly induced during the early regeneration stage when satellite cells became activated, proliferated and started to differentiate, but gradually downregulated later on when the newly formed fibers matured and regeneration was completed in about 10 days (Figure 1M). Consistently, high levels of *Dum* were observed in limb muscles of newborn mice (at the age of 3 days, 5 days and 2 weeks) which displayed active myogenesis, but the level of *Dum* decreased as the neonatal myogenesis ceased after about 2 weeks and remained low as the mice aged (Figure 1N). Moreover, when compared to normal muscles from wild-type mice, higher levels of *Dum* were detected in dystrophic muscles from mdx mice which were featured by a pathologically active degeneration and regeneration [17] (Figure 1O). The above results strongly suggested that *Dum* is associated with active myogenesis *in vitro* and *in vivo*. In addition, *Dum* expression is highly enriched in the activated satellite cells or primary myoblasts freshly isolated from mouse limb muscle compared to the whole muscle itself (Figure 1P), suggesting that its function is related to satellite cell activities but not mature muscle homeostasis.

Dum is a pro-myogenic factor during myoblast differentiation

The early induction of *Dum* expression during C2C12 differentiation suggested that it may be a pro-myogenic factor during myoblast differentiation. To test this notion, we knocked down *Dum* using an siRNA oligo, si*Dum*#1. Successful knockdown (Figure 2A and Supplementary information, Figure S2A) significantly delayed C2C12 differentiation as assessed by examination of several myogenic markers, *myogenin*, *MyHC* and *troponin*, at both RNA (Figure 2B) and protein (Figure 2C) levels during a 4-day differentiation course. The results were also strengthened by immunofluorescence staining for MyHC and troponin proteins in differentiating myotubes on day

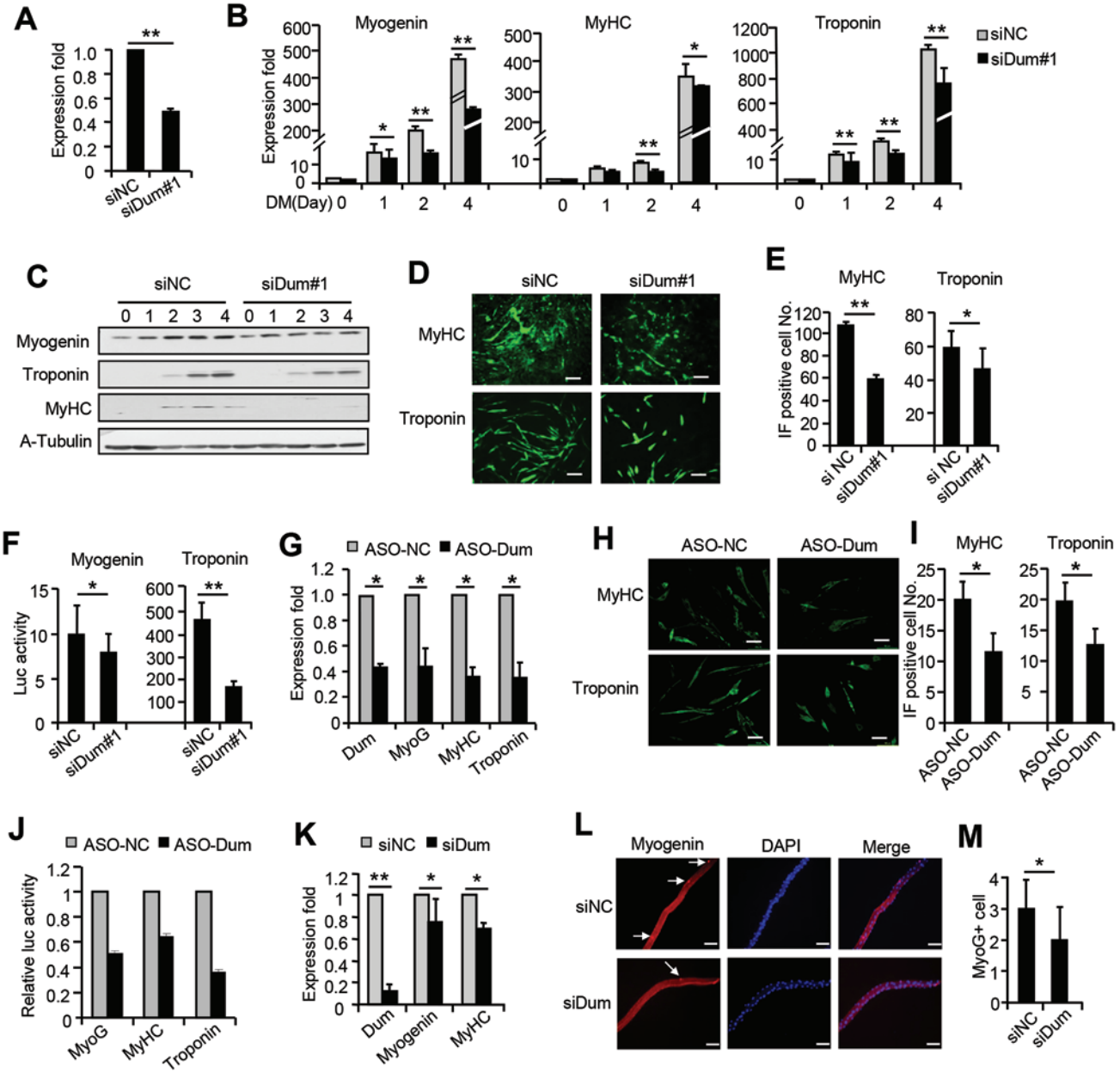

Figure 2 *Dum* functions to promote muscle cell differentiation. **(A)** Knockdown of *Dum* by siRNA oligos in C2C12 cells decreased the expression of *Dum* during a 4-day differentiation course. **(B)** The indicated myogenic genes, *myogenin*, *MyHC* and *troponin* were downregulated in cells from **A**. **(C)** Knockdown of *Dum* decreased the levels of the indicated proteins during a 4-day differentiation course. **(D)** The cells in **A** were visualized on day 2 in differentiation medium (DM). Immunofluorescence staining for MyHC or troponin was performed. **(E)** The number of positively stained cells in **D** was quantified. **(F)** Knockdown of *Dum* in C2C12 cells decreased the luciferase activities of the indicated reporters. **(G)** Knockdown of *Dum* by an ASO oligo in C2C12 cells decreased the expression of *Dum* and the indicated myogenic genes, *myogenin*, *MyHC* and *troponin*. **(H)** The cells from **G** were visualized on day 2 in DM. Immunofluorescence staining for MyHC or troponin was performed. **(I)** The number of positively stained cells in **H** was quantified. **(J)** Knockdown of *Dum* by ASO in C2C12 cells decreased the luciferase activities of the indicated reporters. **(K)** Knockdown of *Dum* in freshly isolated satellite cells decreased the myogenic differentiation. **(L**, **M)** Knockdown of *Dum* in single fibers decreased the satellite cell differentiation as shown by immunofluorescence staining for myogenin. All PCR data were normalized to *GAPDH* mRNA and represent mean ± SD of three independent experiments. All luciferase activity data were normalized to Renillia protein and represent mean ± SD of three independent experiments. **P* < 0.05, ***P* < 0.01. See also Supplementary information, Figure S2.

2 (Figure 2D); the number of positive myotubes was reduced by si*Dum* treatment by 46% and 23%, respectively (Figure 2E). Furthermore, co-transfection of si*Dum* together with a myogenin or troponin luciferase reporter significantly inhibited their luciferase activities as compared to negative control oligos (Figure 2F). To confirm the above results, a second siRNA oligo, si*Dum*#2, was used and the same inhibitory effect was observed by assaying the myogenic RNA expression (Supplementary information, Figure S2B) and reporter activities (Supplementary information, Figure S2C). In addition, since it is still questionable whether siRNAs can efficiently delete nuclear resident lncRNAs, we repeated the above experiments using an optimized phosphorothioate-modified antisense oligodeoxynucleotide (ASO) against *Dum*. Knockdown of *Dum* by the ASO also delayed myogenic differentiation (Figure 2G-2J). Surprisingly, in gain-of-function assay using a *Dum* overexpression plasmid, no impact on myogenic differentiation was observed despite repeated efforts (Supplementary information, Figure S2D-S2G).

To extend our findings in C2C12 cells to a more physiologically relevant setting, we tested the function of *Dum* in freshly isolated satellite cells. In keeping with its pro-myogenic function in C2C12 cells, knockdown of *Dum* by siRNA oligos impaired the myogenic differentiation as shown by the reduced levels of *myogenin* and *MyHC* mRNAs (Figure 2K). These findings were further confirmed in satellite cells associated with freshly isolated single myofiber which serves as an excellent *ex vivo* model. Transfection of si*Dum* oligos impaired satellite cell differentiation capacity as shown by a 33% decrease in the number of myogenin-positive cells per fiber compared to siNC treatment (Figure 2L and 2M).

Loss of Dum delayed CTX-induced muscle regeneration in vivo

The above findings underscored the role of *Dum* in satellite cell function, leading us to believe that it exerts a role in muscle regeneration *in vivo*. To test this notion, we depleted *Dum* in mouse limb muscles during injury-induced regeneration using intramuscular injection of siRNA oligos as described before [17-19]. As illustrated in Figure 3A, the injection of si*Dum* or negative control oligos was performed three times on days 1/4, 2 and 4 post CTX injection and muscles were harvested at the designated times for analyses. Results indicated that injection of si*Dum* oligos led to a significant loss of *Dum* expression along the regeneration course (Figure 3B). Accordingly, the mRNA levels of *Pax7*, *MyoD*, *myogenin* and embryonic *MyHC* (*eMyHC*, a marker for newly formed fibers) were all significantly decreased (Figure 3B); and the protein levels of Pax7, MyoD and mygenin were also reduced (Figure 3C, 43%, 45% and 42%), suggesting a delay of myogenic program. Consistently, by immunofluorescence staining of the muscle sections, the numbers of cells positively stained for Pax7, MyoD, myogenin and eMyHC were evidently reduced (Figure 3D-3G, 60%, 40%, 33% and 44%). Altogether, the above results demonstrated that loss of *Dum* caused a significant delay of injury-induced muscle regeneration *in vivo*.

Dum promotes myogenesis through in cis regulation of Dppa2 transcription

To probe into the mechanisms underlying the pro-myogenic function of *Dum*, we considered its potential regulation on neighboring genes because many lncRNAs are believed to function *in cis* [20]. Indeed, knockdown of *Dum* in C2C12 cells led to a significant change in the expression of 17 out of 23 neighboring genes examined, ranging from 0.1 to 13 folds (Figure 4A and Supplementary information, Figure S3A). Interestingly, the majority (11/17) were upregulated. This finding demonstrated that *Dum* is a strong *in cis* regulator.

Among all the affected genes, *Dppa2* caught our attention because it was reported to regulate *Oct4* which inhibits muscle cell differentiation [21]. Consistently, knockdown of *Dum* by siRNA (Figure 4B) or ASO oligos (Supplementary information, Figure S3B) in C2C12 cells led to an induction of both *Dppa2* and *Oct4* expression. Furthermore, loss of *Dum* in CTX-injured muscles upregulated the expressions of *Dppa2* and *Oct4* through the regeneration course (Figure 4C). In contrast to the upregulation of *Dum* levels, *Dppa2* and *Oct4* expression was gradually downregulated during the early differentiation of both C2C12 cells (Figure 4D) and freshly isolated satellite cells (Figure 4E), suggesting the anti-myogenic nature of *Dppa2*. At a functional level, indeed, knockdown of *Dppa2* by siRNA oligos upregulated the myogenic reporter activities. Furthermore, co-transfection of si*Dppa2* oligos significantly reverted the inhibitory effect of si*Dum* (Figure 4F), suggesting that *Dum* function is probably dependent on *Dppa2*. This was validated in primary myoblasts. si*Dum* oligos inhibited the primary myoblast differentiation, whereas si*Dppa2* promoted it (Figure 4G). Furthermore, in the regenerating muscles, si*Dppa2* treatment was able to rescue the suppressive effect of si*Dum* on regeneration (Figure 4H).

Dum silences Dppa2 expression through recruiting Dnmts to its promoter CpG sites

The above results demonstrated that *Dum* suppresses *Dppa2* transcription upon differentiation. To further elucidate the regulatory mechanisms at the molecular level,

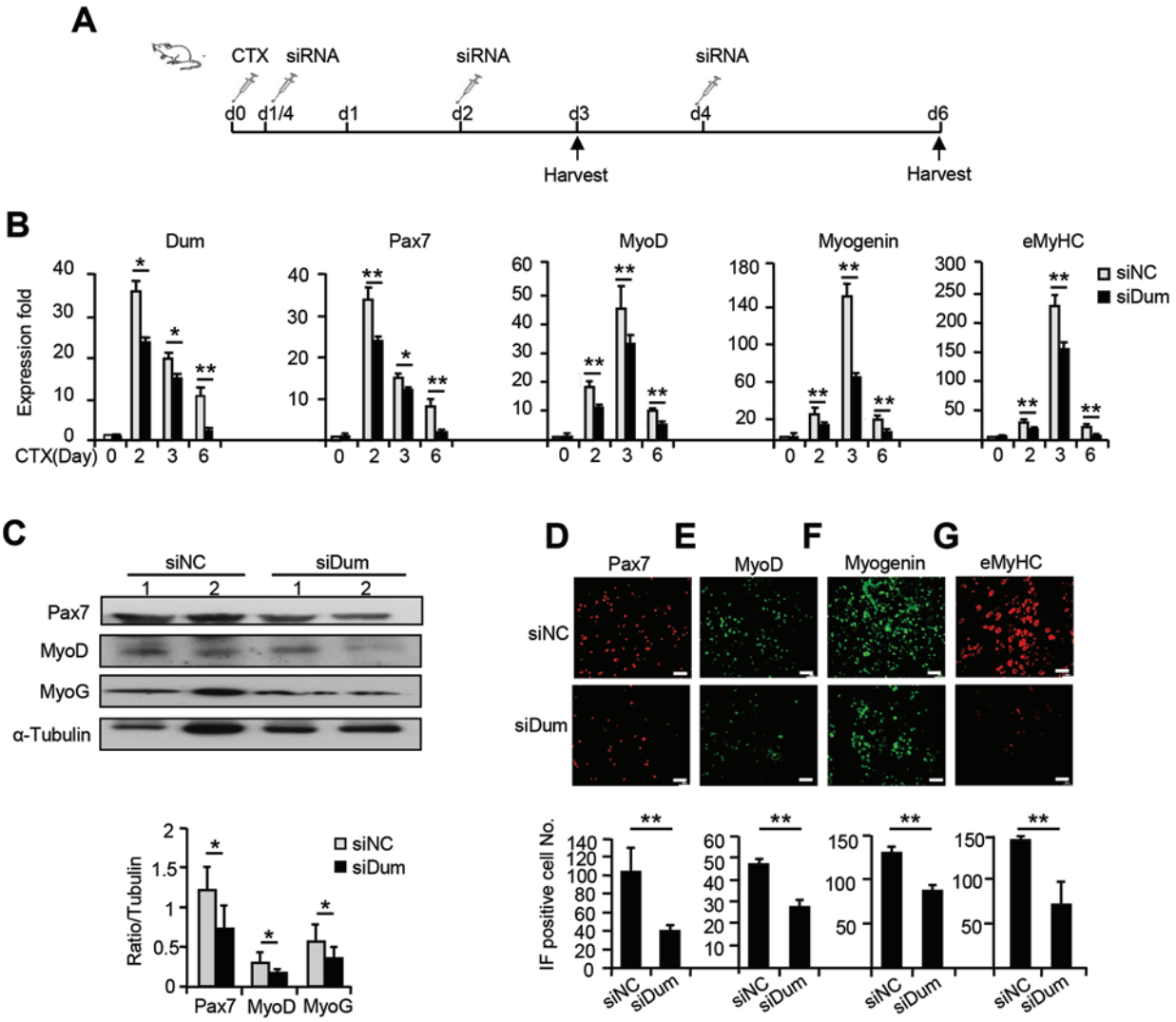

Figure 3 *Dum* knockdown *in vivo* impaired the injury-induced muscle regeneration. **(A)** Injection scheme for siNC or si*Dum* oligos into CTX-injured muscles. *n* = 4 mice for each group. **(B)** *Dum* siRNA injection into CTX-injured muscles decreased the levels of the indicated RNAs at multiple time points after CTX injection. **(C)** Upper panels: *Dum* siRNA injection decreased the levels of the proteins in two representative mice. Lower panel: α-tubulin was used as normalization for the quantification of the western blot band intensity. **(D-G)** Immunofluorescence staining for Pax7, MyoD and myogenin was performed on the injected muscles in **A** on day 3 and eMyHC on day 6. Positively stained cells were quantified. All PCR data were normalized to GAPDH mRNA and represent mean ± SD of three independent experiments. **P* < 0.05, ***P* < 0.01.

we asked how *Dum* modulates *Dppa2* transcription. Although it is still unclear how *Dppa2* transcription is regulated, Ruau *et al.* [22] reported that its level is increased by 5′-Aza-2′-deoxycytidine (5-Aza) treatment in neurosphere cells, leading us to hypothesize that *Dppa2* may be under control by DNA methylation and *Dum* likely silences its expression through regulating the promoter methylation. To confirm that *Dppa2* transcription is regulated by DNA methylation in myoblasts, we treated C2C12 cells with 5-Aza. Expectedly, the treatment induced *Dppa2* expression (Figure 5A); as a positive control, myogenin gene was also induced as previously reported [23]. Several CpG sites were identified in two regions of *Dppa2* promoter by computational prediction (EMBOSS Cpgplot; http://www.ebi.ac.uk) (Figure 5B). Using Bisulfate Genomics Sequencing (BGS) assay, we uncovered that 8 CpG sites were indeed methylated to various degrees upon C2C12 differentiation (Figure 5B). As expected, knockdown of *Dum* reduced the degree of methylation at these CpG sites. Interestingly, the promoters of the other 10 genes (*RP124*, *Dppa4*, *Nfkbiz*, *Cd47*, *Cb1b*, *Senp7 V234*, *Penp*, *Cdc54*, *IFT57* and *Jo3rik*) that

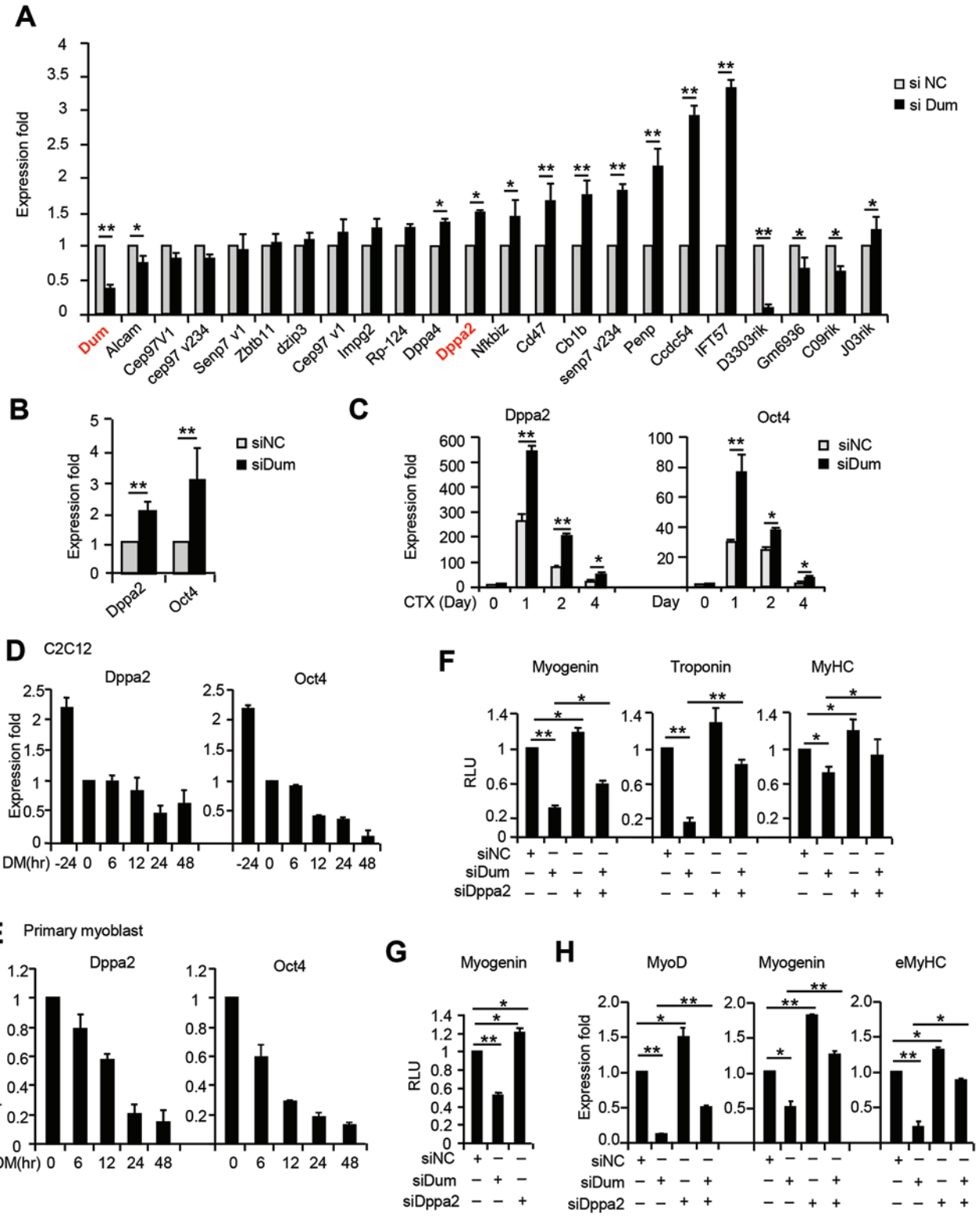

Figure 4 *Dum* regulates *Dppa2* gene expression *in cis*. **(A)** RNAs were isolated from C2C12 cells transfected with siNC or si*Dum* for qRT-PCR measurement of the expression of *Dum* neighboring genes. Expression folds are shown with respect to siNC cells where normalized copy numbers were set to 1. **(B)** Expression of *Dppa2* and *Oct4* in the transfected cells from **A**. **(C)** Expression of *Dppa2* and *Oct4* in regenerating muscle injected with siNC or si*Dum* oligos. **(D, E)** Expression of *Dpppa2* or *Oct4* during C2C12 (**D**)or primary myoblast **(E)** differentiation. **(F, G)** C2C12 cells (**F**) or primary myoblasts **(G)** were

transfected with the indicated siRNA oligos and the myogenic reporter. Luciferase activities were determined at 48 h post transfection. Relative luciferase unit (RLU) is shown with respect to siNC cells where normalized luciferase values were set to 1. **(H)** The indicated siRNA oligos were injected into the CTX-induced regenerating muscle and the expression of the myogenic markers were meansured 3 days after the injection. The data represent mean ± SD of three independent experiments. All PCR data were normalized to *GAPDH* mRNA and represent mean ± SD of three independent experiments. All luciferase acitivity data were normalized to Renillia protein and represent mean ± SD of three independent experiments. **P* < 0.05, ***P* < 0.01. See also Supplementary information, Figure S3.

were upregulated upon *Dum* knockdown (Figure 4A) were not subjected to methylation by BGS assay (data not shown), suggesting a unique regulatory mechanism of *Dum* on *Dppa2*.

The above results demonstrated that *Dum* indeed modulates *Dppa2* promoter methylation, leading us to speculate that *Dum* is involved in targeting or association with DNMTS. It is known that *de novo* enzymes Dnmt3a and Dnmt3b could form complexes with the major maintenance enzyme Dnmt1 to cooperate in establishing and maintaining genomic methylation patterns [24]. To test whether *Dum* interacts with this complex, we first performed RNA immunoprecipitation (RIP) assay using antibodies against Dnmt1, Dnmt3a or Dnmt3b. Notably, all three antibodies retrieved significant amounts of *Dum* RNAs, with Dnmt1 pulling down the highest level (6-fold increase compared to IgG control); as a negative control, Xist RNAs were not retrieved (Figure 5C), indicating a specific interaction between Dnmts and *Dum*. To strengthen this finding, we further performed RNA pull-down assay using *in vitro*-generated biotinylated full-length (FL) *Dum* transcripts. Consistently, as shown in Figure 5D, *Dum* transcripts pulled down substantial amounts of Dnmts. As negative controls, beads alone or GFP transcripts did not retrieve Dnmts. To further map the binding domain, a series of deletion mutants of *Dum* were generated and tested for the binding with Dnmts. Interestingly, deletion of the 3′ fragment (F1+2) did not affect the binding efficiency with Dnmts; further deletion of the middle domain (F1) resulted in reduced binding with Dnmt1 and 3a and loss of binding with Dnmt3b; and the middle (F2) or 3′ domain (F3) alone could not bind with any Dnmt, indicating that both the 5′ and the middle domains are required for effective binding with Dnmts. Furthermore, we performed ChIP-PCR assays to show that knockdown of *Dum* significantly impaired the binding of Dnmts to the above identified two CpG regions (Figure 5E and Supplementary information, Figure S4A), confirming that *Dum* is critical for the association of Dnmts with *Dppa2* promoter. The above findings were further validated in regenerating muscles by performing *in vivo* RIP and ChIP assays. The association of Dnmt3a and Dnmt1 with *Dum* was indeed detected on *Dppa2* promoter in the muscles *in vivo* (Figure 5F), and the occupancy of Dnmts on *Dppa2* promoter was markedly decreased by intramuscular si*Dum* treatment (Figure 5G).

Altogether, our data suggested that *Dum* mainly functions *in cis* to silence *Dppa2* expression upon myogenic differentiation, which explains why ectopic expression of *Dum* had no detectable impact on myogenic differentiation (Supplementary information, Figure S2). To further confirm its *cis* acting nature, the *in vitro*-transcribed *Dum* full-length transcripts were transfected into C2C12 cells. Successful overexpression of *Dum*, however, did not change the expression level of *Dppa2* (Figure 5H); consistently, no exogenous *Dum* transcripts were detected on the endogenous *Dppa2* promoter by pulling down biotin-labeled *Dum* transcripts (Figure 5I). Interestingly, a substantial degree of complementarity was found between *Dum* sequence (1 285-1 414) and *Dppa2* promoter (Supplementary information, Figure S4B), suggesting that the endogenous *Dum* probably associates with *Dppa2* promoter through direct RNA:DNA interaction (Supplementary information, Figure S4C). Indeed, using Chromatin Isolation by RNA Purification (ChIRP) assay [25] with both odd and even tiling oligos against *Dum*, we were able to specifically retrieve substantial amount of endogenous *Dum* transcripts from the above tested *Dppa2* promoter regions 1 and 2 but not a nearby region 3 (Figure 5J and Supplementary information, Figure S4D).

To further explore how *Dum* orchestrates *Dppa2* promoter activity over such a long distance (~2 Mb), we thought of chromatin looping that has been demonstrated between transcriptional regulatory elements and promoters [26]. As evident from the literature and argued by Taberlay *et al*. [27], the available genome-wide assays for chromatin conformation analyses are unreliable for interpreting connectivity at distances >100 kb. However, the chromatin occupancies of the cohesin complex, which facilitates enhancer-promoter looping, may infer such interactions [27-29]. Therefore, we assessed the occupancy of Rad21, a member of cohesion complex, and Nipbl, a cohesin-loading factor. We found significant enrichment of both factors on *Dum* locus and *Dppa2* promoter (Figure 5K and 5L), suggesting that the long-range chromatin interaction may occur between *Dum* and *Dppa2* loci. Furthermore, knockdown of *Rad21* or *Nipb1*

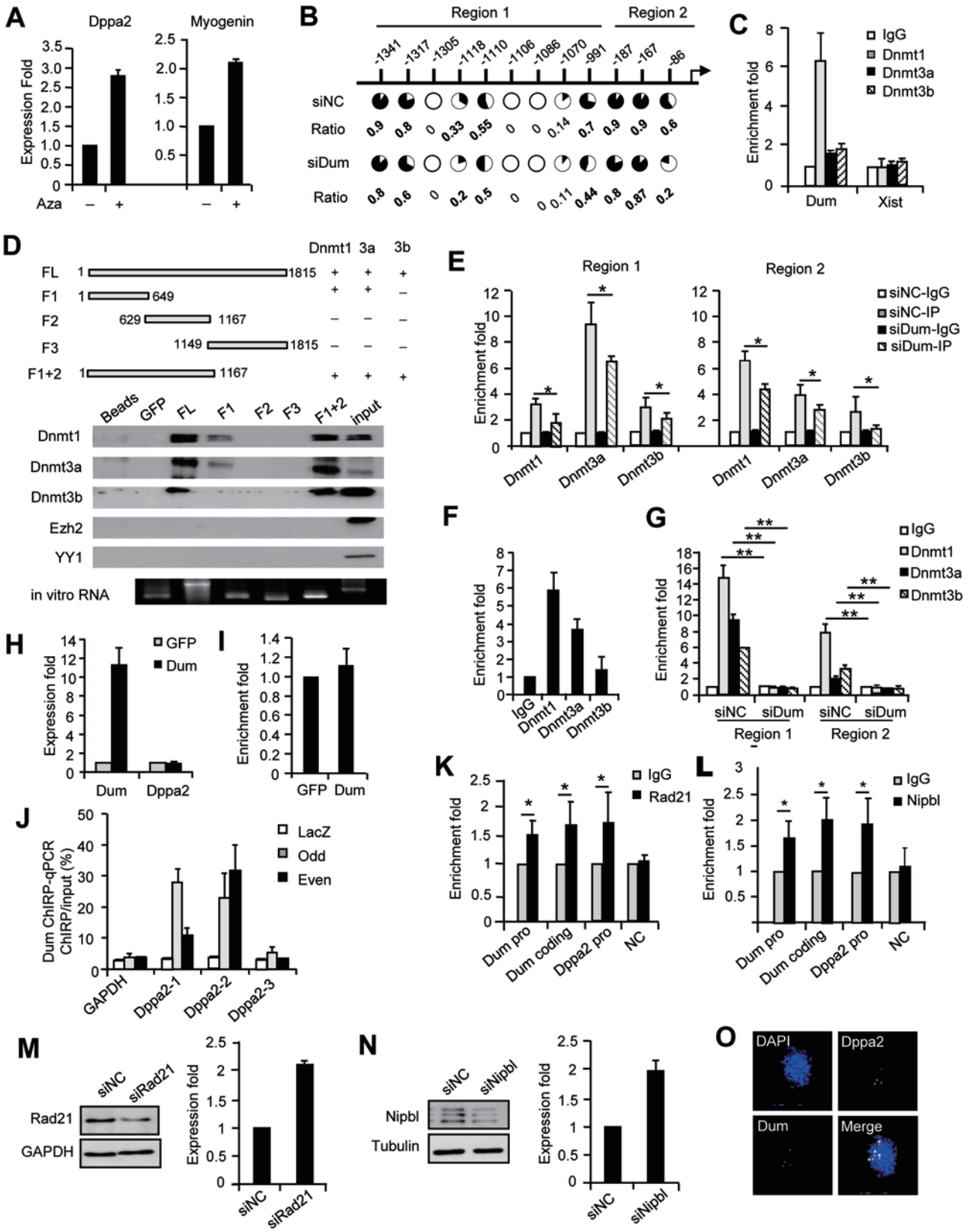
A
Dppa2
Myogenin
Expression Fold
Aza
B
Region 1
Region 2
siNC
Ratio
siDum
C
IgG
Dnmt1
Dnmt3a
Dnmt3b
Enrichment fold
Dum
Xist
D
Dnmt1 3a 3b
FL
F1
F2
F3
F1+2
Beads
GFP
input
Ezh2
YY1
in vitro RNA
E
siNC-IgG
siNC-IP
siDum-IgG
siDum-IP
F
G
H
GFP
Dum
Dppa2
I
J
LacZ
Odd
Even
Dum ChIRP-qPCR
ChIRP/input (%)
GAPDH
Dppa2-1
Dppa2-2
Dppa2-3
K
Rad21
Dum pro
Dum coding
Dppa2 pro
NC
L
Nipbl
M
siNC
siRad21
N
siNipbl
O
DAPI
Dppa2
Dum
Merge

Figure 5 *Dum* interacts with Dnmts to induce *Dppa2* promoter methylation. **(A)** C2C12 cells were treated with or without 5-Aza; the expression of *Dppa2* or *myogenin* was decreased as shown by qRT-PCR. **(B)** CpG sites were identified in two regions (region 1, −1 308 to −1 166 and region 2, −185 to −47) of *Dppa2* promoter and the methylation was measured using bisulfate genomic sequencing in siNC- or si*Dum*-treated cells. The degree of methylation was decreased by si*Dum* as shown by percentage of the methylated cytosines from 10 randomly sequenced colonies. **(C)** Dnmt1, Dnmt3a and Dnmt3b bound to *Dum* but not *Xist* in C2C12 cells as revealed by RIP assay. **(D)** *In vitro*-generated biotin-labeled full-length or the deletion fragments were used to pull down Dnmts. No binding to Ezh2 and YY1 was detected (negative controls). **(E)** Knockdown of *Dum* by siRNA oligos in C2C12 cells decreased the enrichment of Dnmts on *Dppa2* promoters by ChIP-PCR assay. **(F)** Dnmt binding to *Dum* was detected in CTX-induced regenerating muscle by *in vivo* RIP assay. **(G)** Knockdown of *Dum* in regenerating muscle decreased the enrichment of Dnmts on *Dppa2* promoters by *in vivo* ChIP-PCR assay. **(H)** Transfection of the *in vitro*-transcribed *Dum* transcripts led to successful overexpression of *Dum* as compared to transfection of *in vitro*-transcribed GFP transcripts. It, however, had no effect on *Dppa2* expression. **(I)** The ectopic *Dum* or control *GFP* transcripts from **H** were not detected on *Dppa2* promoter. **(J)** *Dum* ChIRP with both even and odd antisense oligos retrieved a significant amount of genomic DNAs corresponding to *Dppa2* promoter regions 1 and 2 as defined in **B** but not in a third region (−1 589 to −1 411) and *GAPDH* locus. *LacZ* ChIRP retrieved no signal. **(K, L)** The enrichment of Rad21 or Nipbl on *Dum* locus (promoter or coding regions) or *Dppa2* promoter region was detected by CHIP-PCR assay. A negative control (NC) region (20 kb upstream of *Dum* locus) showed no enrichment for the above factors. **(M, N)** Knockdown of Rad21 or Nipbl by siRNA oligos increased the expression of *Dppa2* in C2C12 cells as revealed by qRT-PCR. **(O)** Double DNA FISH of *Dum* (red) and *Dppa2* (green) genomic loci in C2C12 cells. White stars indicate the co-localized loci from a tetraploid cell. All PCR data were normalized to *GAPDH* mRNA and represent mean ± SD of three independent experiments. **P* < 0.05, ***P* < 0.01. See also Supplementary information, Figure S4.

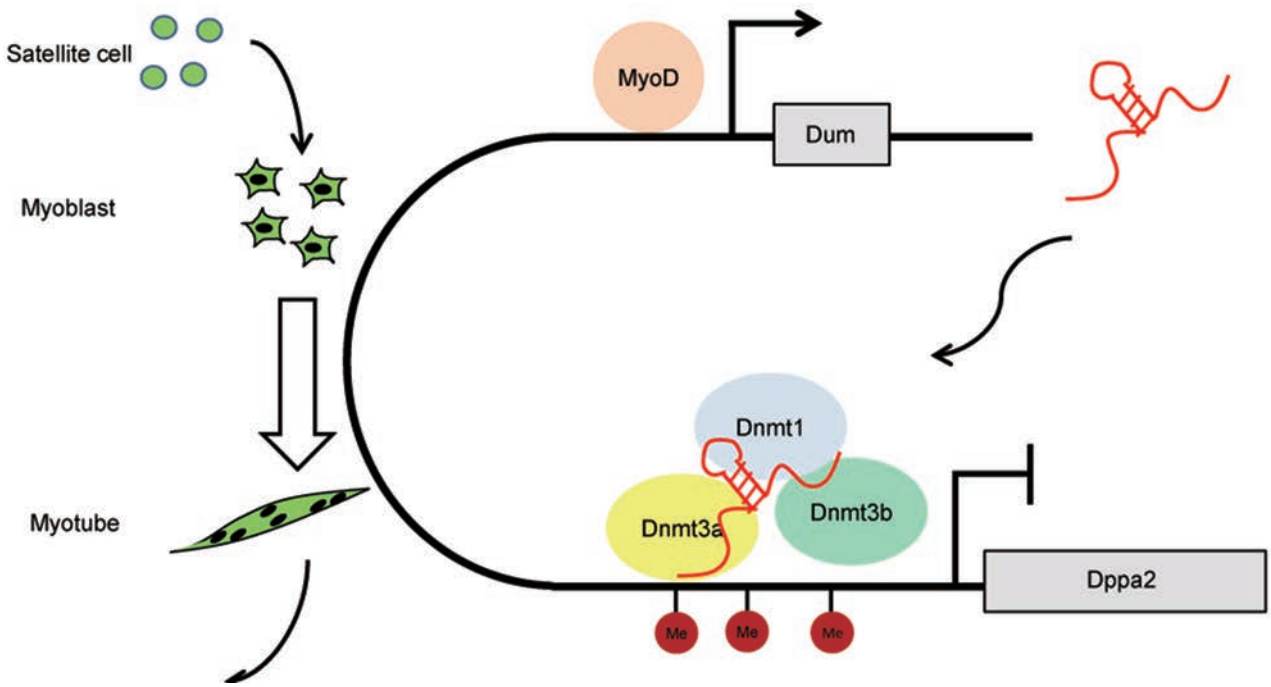

Figure 6 Proposed model of *Dum* regulation of *Dppa2* expression. The model depicts the role of the MyoD-*Dum*-*Dppa2* regulatory axis in myogenic differentiation and regeneration. *Dum* expression is induced by MyoD upon myoblast differentiation. The intrachromosomal looping between *Dum* and *Dppa2* loci juxtaposes *Dum* transcripts to *Dppa2* promoter; subsequently, *Dum* interacts with and recruits Dnmts to *Dppa2* promoter, leading to CpG site hypermethylation and gene silencing.

by siRNA oligos led to an induction of *Dppa2* expression (Figure 5M and 5N), confirming the involvement of cohesin complex in *Dppa2* silencing. To further strengthen the above results, we visualized the localization of the *Dum* locus and *Dppa2* promoter by double DNA FISH using two probes that recognize either the *Dum* or *Dppa2*

promoter. As expected, we found that these two loci were spatially colocalized in ~60% cells examined (Figure 5O). Meanwhile, the centromere region recognized by a negative control probe showed no colocalization with *Dum* locus in all cells examined (Supplementary information, Figure S4E).

Discussion

In this study, we unraveled the novel functional roles of a lncRNA, *Dum*, in regulating skeletal muscle cell differentiation and muscle regeneration. As illustrated in Figure 6, we demonstrated that *Dum* promotes myogenic differentiation by silencing *Dppa2* expression *in cis*. Mechanistically, it promotes DNA methylation of *Dppa2* promoter by binding to its promoter and recruiting Dnmts.

Although a large number of lncRNAs are pervasively identified from mammalian genomes, only a minority have been understood at the functional level [4]. The existent studies from about 100 characterized lncRNAs support a major role in epigenetic regulation through interacting with histone modifiers. *Dum* represents one of the few lncRNAs that modulate DNA methylation and the first identified to interact with both *de novo* methylation and maintenance Dnmts. Our findings suggest a novel model of silencing *Dppa2* locus in which *Dum* recruits Dnmts through intrachromosomal looping. *Dum* appears to be a strong *in cis* regulating factor since a range of neighboring genes were all changed by *Dum* knockdown. However, *Dppa2* seems to be the only one regulated by *Dum* through modulating its promoter methylation. The other genes may be controlled through other mechanisms or indirectly through other factors. It is still unclear to us whether *Dum* is necessary for the intrachromosomal looping formation between *Dum* locus and *Dppa2* promoter. Most likely, it is not involved in the looping formation because ectopic expression of *Dum* had no effect on *Dppa2* promoter repression, suggesting that *Dum* acts co-transcriptionally when it is in close contact with *Dppa2* promoter; *Dum* expression is probably induced by the pre-existing looping. Further studies are needed to shed light on this aspect. This also sets *Dum* apart from *Kcnqu1* ot1 lncRNA which functions as a molecular hinge to link the *Kcnq1* promoter and *KvDMR1* DNAs together and a scaffold for a long-range intrachromosomal loop [30]. Our results from ChIRP assay also indicated that *Dum* anchors to *Dppa2* CpG regions through directly binding to the two regions identified, suggesting that it acts as a tethering molecule to recruit Dnmts. This can be related to the recently identified *ecCEBPA* which anchors DNMT1 to the locus [9], suggesting that lncRNA-Dnmt interaction may be a general phenomenon. However, in the case of *ecCEBPA*, DNMT1 is sequestrated not targeted to the locus. Furthermore, unlike ecCEBPA which interacts with Dnmt1 only, *Dum* interacts with both maintenance and *de novo* DNMTs, ie, Dnmt1, Dnmt3a and Dnmt 3b. This suggests that *Dum* is possibly involved in the cooperation between the DND methyltransferases probably by functioning as a scaffolding molecule. All three Dnmts seem to bind the 1-1 167 domain of *Dum*; further deletion of the middle domain abolished Dnmt3b binding while retained binding to Dnmt1 and Dnmt3b, suggesting that this fragment is critical for Dnmt3b interaction. In the future it will be interesting to map the exact interacting interface even structural element of *Dum* with each Dnmt.

Much of our understanding of epigenetic regulatory network in skeletal myogenesis is focused on the level of chromatin and relatively less is known on the DNA methylation. Our study underscores the importance of promoter CpG methylation in skeletal myogenesis; it is also the first to show that *Dppa2* is a regulator of myogenesis. *Dppa2* was previously known to be highly enriched in pluripotent cells with decreased expression in differentiated cells [12]. Our results indicate that analogous to its function in ES cells, *Dppa2* might play a role in maintenance of the undifferentiated state and proliferation of myoblast cells. Nothing was known how *Dppa2* expression is downregulated in differentiated cells; our findings thus provide the first line of evidence to show DNA methylation is responsible for its silencing. This mechanism may work beyond myoblasts cells to explain how *Dppa2* is downregulated during ES cell differentiation or in other cell types. In addition to its function in the myoblast differentiation, it is likely that *Dum* also plays a role in the other steps of satellite cell function. *In vivo* treatment of si*Dum* in the injured muscles decreased the *Pax7* and *MyoD* expression and the number of Pax7- and MyoD-positive satellite cells (Figure 3). This strongly suggested that knockdown of *Dum* may also impact satellite cell activation/proliferation or self-renewal capacity. Future exploration of these aspects will lead to a more comprehensive picture of how *Dum* functions in muscle stem cells and muscle regeneration.

Materials and Methods

Cell lines

Mouse C2C12 myoblasts and 10T1/2 cells were obtained from ATCC and cultured in DMEM supplemented with 10% fetal bovine serum (FBS), 2 mM L-glutamine, 100 U/ml penicillin and 100 μg of streptomycin (1% Pen/Strep) at 37 °C in 5% CO_2. For myogenic differentiation experiment, cells were seeded in 100 mm plates and when reaching 90% confluence they were shifted

to DMEM containing 2% horse serum (HS). 10T1/2 cells were cultured in DMEM supplemented with 10% FBS and induced to myogenic differentiation after MyoD transfection by shifting to DMEM containing 2% HS. For 5-Aza treatment, C2C12 cells were treated with 10 mM 5-Aza (Zymo research, CA, USA) for 72 h. Total RNAs were then extracted for RNA analysis.

Primary myoblast isolation

Primary myoblasts were isolated from ~1-week-old mouse muscles as described before [16, 17]. Briefly, total hind limb muscles (3-6 mice per group) were digested with 5 mg/ml type IV collagenase (Life Technologies, Carlsbad, CA, USA) and 1.4 mg/ml dispase II (Life Technologies) for 0.5 h, and cell suspensions were filtered through 70 and 40 μm cell strainer, respectively, then pre-plated for 1 h. Non-adherent cells were centrifuged and cultured on gelatin-coated plates (Iwaki, Japan) in F10 medium (Life Technologies) supplemented with 20% FBS and basic fibroblast growth factor (bFGF) (Life Technologies, 25 ng/ml). After removing fibroblasts by pre-plating, primary myoblast cells were cultured in F10/DMEM medium (1:1) supplemented with 20% FBS and bFGF.

Cell fractionation

For fractionation assay, cytoplasmic and nuclear RNAs were extracted from C2C12 myoblasts as previously described [13]. Briefly, cells were harvested after trypsinization and washed with PBS twice. Cell pellet was then resuspended in RSB buffer (10 mM Tris, pH 7.4, 10 mM NaCl, 3 mM $MgCl_2$) and incubated on ice for 3 min followed by centrifugation at 4 °C. The pellet was then resuspended in RSBG40 buffer (10 mM Tris, pH 7.4, 10 mM NaCl, 3 mM $MgCl_2$, 10% glycerol, 0.5% Noidet P-40, 0.5 mM dithiothretol and 100 U/ml rRNasin) followed by centrifugation. The supernatant was transferred to a new tube as cytoplasmic fraction; the pellet was resuspended in RSGB40 buffer with 1/10 volume of detergent (3.3% sodium deoxycholate and 6.6% Tween 40) followed by centrifugation. The supernatant was saved as cytoplasmic fraction. The pellet was used as nuclear fraction. RNAs were extracted from both fractions using Trizol.

Single-fiber isolation and use

Single-fiber isolation was performed as previously described [31]. Briefly, two of extensor digitorum longus (EDL) muscles were excised from C57BL/6 mice and digested in 1 ml of DMEM containing 500 U/ml collagenase II, 10% HS, 1% Pen/Strep at 37 °C with gentle agitation for 75 min. The digestion solution is then transferred into 20 ml of pre-warmed DMEM containing 10% HS, 1% Pen/Strep, 20 mM HEPES, pH 7.3, in HS-precoated 100 mm Petri dish. Single fibers were liberated by gently triturating the digested EDL muscles against the edge of Petri dish using a fire-polished Pasteur pipet with wide tip. Once around 100 fibers have fallen off, the dishes were placed back to incubator. Individual, healthy (non-shrinking) fibers were transferred to a new HS-coated 100 mm dish using the HS-coated P1000 tips every 15-25 min and the transfer was repeated three times to remove debris and the interstitial cells from fibers. Finally, 50 single fibers were transferred to each 35 mm dish with 1 ml of Ham's F10 medium containing 10% HS, 0.05% chick embryo extract, and cultured in suspension. Transfection was performed on the same day. 50 pmol siRNA or 2 μg plasmid is mixed with 10 μl Lipofectamine 2000 in 50 μl Opti-MEM I and incubated for 20 min before adding to myofibers and incubated at 37 C overnight. Generally, every 24 h, 50% of the medium was replaced with Ham's F10 medium with 20% FBS. For differentiation, 24 h after transfection, 50% of the medium was replaced with DMEM containing 2% HS and incubated for 3 days. For immunofluorescence staining, fibers were fixed with 2% paraformaldehyde in medium and stained using anti-Pax7 or anti-myogenin antibodies. The number of Pax7- or myogenin-positive cells was quantified from at least 20 fibers.

DNA constructs

To generate a *Dum* expression plasmid, the full-length coding region of *Dum* was amplified and cloned into pcDNA3.1(+) vector (Invitrogen) using *Nhe*I and *Kpn*I sites. The expression vectors for the truncated mutants were generated by amplifying the corresponding fragment and cloned into the pcDNA3.1(+) vector. For *in vitro* transcription, the DNA was subcloned into pBluescript vector using *BamH*I and *Kpa*1 sites. Sequences of the primers used can be found in Supplementary information, Table S1. Myogenin, MyHC and troponin luciferase reporters (MyoG-Luc, MyHC-Luc and Troponin-Luc) were used as described [32]. Renilla luciferase reporter was obtained from Promega and used according to the manufacturer's instructions.

Sodium bisulfite modification and genomic sequencing

Genomic DNA was modified by sodium bisulfate as described previously [33, 34]. Genomic DNA was extracted from cultured cells, using the DNA-easy kit (Qiagen, Hilden, Germany) according to the manufacturer's instructions. 2 μg of DNA was bisulfate modified at 50 °C overnight. Bisulfate-modified DNA was purified with the Wizard DNA Clean-up system (Promega) and eluted in water. To get the bisulfate-specific genomic PCR products, 1 μl (~50 ng) bisulfate-modified DNA was applied in a 25 reaction volume by HotStarTaq DNA Polymerase kit (Qiagen). DNA fragments were gel purified with the QIAquick Gel Extraction kit (Qiagen) and sequenced (BGI).

Double DNA FISH

Double DNA FISH was modified as described [35]. Position-specific probes were obtained from BAC clones of RP23-361N24 for Dppa2 and RP24-264D19 for *Dum* (http://www.chori.org/bacpac/). DNA probes were synthesized with nick translation kit (Abbotte, IN, USA) and spectrum green or orange dUTP for direct labeling. Mouse chromosome 16 centromeric probe labeled with FITC was purchased from ID Labs Inc (London, UK). *Dum* and Dppa2 DNA FISH probes were labeled with Alexa Fluor 488 (green) and 594 (red) by Nick Translation, respectively. C2C12 cells were treated with colcemid (50 ng/ml, Invitrogen) for 3 h. The trypsinized single cells were then swollen by 75 mM KCl treatment for 20 min at 37 °C and fixed by cold methanol/acetic acid (v/v, 3:1) for 5 min three times. Cells were denatured at 75 °C for 5 min in prewarmed 2× SSC and 70% deionized formamide (pH 7.0). Next, cells were hybridized overnight at 37 °C with denatured DNA probes (73 °C for 5 min). After hybridization, two washes of 10 min at 73 °C with 0.4× SSC/50% deionized formamide, pH 7.0, followed by two washes of 5 min at ambient temperature with 2× SSC/50% deionized formamide. Slides were then mounted with ProLong Gold antifade reagent with DAPI. Pictures were taken with a Zeiss microscope with 100 oil lens. Colocalization signals

were analyzed in double-positive cells.

ChIP assay

ChIP assays using chromatins from C2C12 myoblasts or myotubes were performed as previously described [16, 36] using 5 μg of antibodies against MyoD (Santa Cruz Biotechnology, TX, USA), DNMT3A/3B (Abcam, Cambridge, UK), DNMT1 (Abcam), Rad21 (Abcam) and NIPBL (Bethyl, TX, USA) or isotype IgG (Santa Cruz Biotechnology) used as a negative control. Genomic DNA pellets were resuspended in 20 μl of water. qRT-PCR was performed with 1 μl of immunoprecipitated material with SYBR Green Master Mix (Life Technologies). Relative enrichment is calculated as the amount of amplified DNA normalized to input and relative to values obtained after normal IgG immunoprecipitation, which were set as 1. Primers used are listed in Supplementary information, Table S1.

Oligonucleotides

siRNA oligos were obtained from Ribobio (Guangzhou, China). The 19-nucleotide siRNA duplexes against mouse MyoD coding region (siRNA, 5′-GCCUGAGCAAAGUGAAUGA-3′) or coding region (siRNA, 5′-CAGCAGACGACUUCUAUGA-3′), *Dum* coding region (siRNA, 5′-GAATGAUCGUCCCAUGUUA-3′) or coding region (siRNA, 5′-GAAAGAGAAUCCAAGGUAA-3′) or coding region (siRNA, 5′-GAGAGAAACUGGUAGAUAU-3′), Dppa2 coding region (siRNA, 5′-GCAGAUGCCUGUCUUACAA-3′) or coding region (siRNA, 5′-CGGAGACACUCCUAUUCUA-3′), Rad21 coding region (siRNA 5′-GCAGCUUAUAAUGCCAUUA-3′) or coding region (siRNA, 5′-CCAGUACAAAGAUGACAAU-3′) or coding region (siRNA, 5′-GCGGUAUAUUAGAUGACAA-3′), NIPBL coding region (siRNA, 5′-GCAGAUGCCUGUCUUACAA-3′) or coding region (siRNA, 5′-GCAUCCGAGUCUAAUGUUU-3′) or coding region (siRNA, 5′-GCACCAAUGCUCGGAACAA-3′) and scrambled oligos were obtained from Ribobio. In each case, 50 μM oligos were used for transient transfections into cells. 2′-o-methylated and phosphorothioate-modified ASO oligo against *Dum* or scrambled oligo were synthesized at Ribobio. 100 nM oligo was introduced into C2C12 cells with Lipofectamine 2000 (Life Technologies).

RT-PCR and northern blotting analysis

Total RNAs from cells were extracted using TRIzol reagent (Life Technologies) according to the manufacturer's instructions and cDNAs were prepared using M-MLV (Moloney Murine Leukemia Virus) Reverse Transcriptase (Life Technologies) and Oligo (dT) 20 primer. Analysis of mRNA expression was performed with SYBR Green Master Mix (Life Technologies) as described on an ABI PRISM 7900HT Sequence Detection System (Life Technologies) using GAPDH for normalization [37]. For northern blotting analysis, sense RNA probe was synthesized by MAXIscript T7 kit (Ambion) with pBluescript-*Dum* DNA linearized with *Kpn*I while antisense RNA probe was synthesized by MAXIscript T3 kit (Ambion) with *BamH*I-linearized DNA. All RNA probes were labeled by UTP [α-32P] (Perkin Elmer).

RNA FISH

In situ hybridyzation was performed following the protocol from Dr Prasanth KV [38]. Biotin-labeled sense and antisense RNA probes were synthesized with linearized pBluscript-*Dum* DNAs (*Kpn*I/*BamH*I digested) and MAXIscript T7/T3 *In vitro* transcription kit, respectively (Invitrogen, Carlsbad, CA, USA), and Biotin RNA labeling Mix (Roche, Rotkreuz, Germany). Cells were fixed with 2%-4% freshly prepared paraformaldehyde (in 1× PBS, pH 7.2) for 15 min at room temperature (RT). The cells were permeabilized with 0.2%-0.5% Triton X-100, 2 mM VRC (NEBiolabs) on ice for 5-10 min and then washed 2 times in 2× SSC for 10 min. 200 g or more of the probe and yeast tRNA (20 μg; Sigma) were lyophilized and redissolved in 10 μl deionized formamide (Ambion) and denatured at 75-100 °C for 10 min and immediately chilled in ice for 3-5 min. 10 μl of hybridization buffer was added to each reaction to make a final hybridization cocktail of 20 μl per coverslip. Coverslips were incubated at 37 °C overnight in a humidified chamber. After hybridization, coverslips were washed in 2× SSC, 50% formamide (pH 7.2) for 3× 5 min at 42 °C, 2× SSC (pH 7.2) for 3 5 min at 42 °C, 1× SSC (pH 7.2) for 3× 5 min at 42 °C and 4× SSC for 2× 10 min at RT. After washing with 0.2× SSC at 65 °C for 1 h, Cy3-labeled streptavidin was added to cells for 1 h at RT. After washing three times with PBS, cells were then mounted with prolong Gold antifade reagent with DAPI (Invitrogen, Carlsbad, CA, USA) and images were captured with Zeiss microscope with 63× oil lens.

RNA pull-down assay

RNA pull-down and deletion mapping were performed as described [39]. Briefly, biotinylated RNAs were prepared using MAXIscript T7/T3 *In vitro* transcription kit (Life Technologies) and Biotin RNA labeling Mix. The above RNAs were denatured at 90 °C for 2 min and then denatured with RNA structure buffer (Life Technologies) at RT for 20 min. 5×10^6 C2C12 cell pellets were treated with 20% nuclear isolation buffer (1.28 M sucrose; 40 mM Tris-HCl, pH 7.5; 20 mM $MgCl_2$; 4% Triton X-100) with 1× Complete Protease Inhibitor Cocktail (PIC, Roche). Nuclei were collected by 2 500× *g* centrifugation for 15 min. Nuclear pellet was resuspended in 1 ml RIP buffer (150 mM KCl, 25 mM Tris, pH 7.4, 0.5 mM DTT, 0.5% NP-40, 1 mM PMSF and 1× PIC) and sonicated with three cycles (30 s interval, 30 s sonication) using Bioruptor (Diagenode, Liege, Belgium). After centrifugation at 13 000 RPM for 10 min to remove nuclear membrane and debris, 1 mg of C2C12 nuclear extract was then mixed with 3 μg of denatured RNA, and incubated at RT for 1 h. 30 μl washed streptavidin agarose beads (Life Technologies) were added to each pull-down reaction and further incubated at RT for 1 h. Beads were pelleted and washed for five times in Handee spin columns (Pierce, IN, USA) using RIP buffer. The resulting beads were boiled in loading buffer to retrieve the proteins which were then detected by standard western blotting technique. For *in vivo* pull-down, the muscle tissue was collected in nuclear isolation buffer and biotin IPs were performed as above described.

RIP assay

RIP was also performed as described [39]. In short, C2C12 cells were crosslinked with 1% formaldehyde and collected for lysis by RIPA buffer (50 mM Tris, pH 7.4, 150 mM NaCl, 1 mM EDTA, 0.1% SDS, 1% NP-40, and 0.5% sodium deoxycholate, 0.5 mM DTT, 1 mM PMSF, 1× proteinase inhibitor cocktail and 1% RNaseOut). The lysate was incubated with specific antibodies or IgG control overnight. The RNA/protein complex was recovered with protein G Dynabeads and washed with RIPA buffer several

times. After reverse crosslink with proteinase K at 45 C for 45 min, RNA was recovered with Trizol and analyzed by RT-PCR.

RNA-biotin-based pull-down assays for the detection of RNA-targeted genomic regions

RNA pull-down assay for detecting of genomic DNA was also performed as described [40]. In short, biotinylated RNAs were prepared using MAXIscript T7 *In vitro* transcription kit (Life Technologies) and Biotin RNA labeling Mix (Roche). The resultant transcripts were DNase treated and dephosphorylated by using Antarctic phosphatase (New England BioLabs). C2C12 cells were transfected with the biotinylated RNAs (70-100 nM of final concentration) with Lipofectamine 2000 (Life Technologies). 24 h following transfection, the treated cultures were crosslinked by adding formaldehyde directly to tissue culture media to a final concentration of 1% for 10 min and stopped by the addition of glycine to a final concentration of 0.125 M. The extracted genomic DNA (200 µl eluent) is then used to detect promoter-specific transcripts with the biotin-linked pull-down assay. Genomic DNA was isolated and exposed to avidin magnetic beads. The final elutes, following the binding of the biotin linked RNAs with the avidin magnetic beads and washing, then were PCR amplified.

Chromatin isolation by RNA purification

CHIRP was performed as described [25]. The antisense probes (20 nucleotides in length) were designed and divided into odd and even pools. C2C12 cells were harvested and cross-linked by 1% glutaraldehyde and sonicated for 4 h by Bioruptor sonicator. Probe pool and cell lysates were then incubated at 37 °C for 4 h. Magnet beads were added to pull down probes and separated with magnet strip. RNAs isolated with Trizol were reverse transcribed into cDNA by M-MLV reverse transcriptase. RNA retrieval was calculated by the percentage of pull-down RNA over input. DNA isolated by phenol-chloroform-ethanol precipitation was used for qRT-PCR. DNA binding enrichment was represented by the percentage of the pull-down DNA over input DNA.

Immunoblotting and immunostaining

For western blot analysis, total cell extracts were prepared and used as previously described [32, 41, 42]. The following dilutions were used for each antibody: Pax 7 (Developmental Studies Hybridoma Bank; 1:2 000), MyoD (Santa Cruz Biotechnology; 1:2 000), myogenin (Santa Cruz Biotechnology; 1:2 000), troponin (Sigma; 1:2 000), MyHC (Sigma; 1:2 000), Rad21 (Abcam; 1:2 000), Nibpl (Bethyl; 1:2 000), α-tubulin (Sigma; 1:5 000), GAPDH (1:5 000; Santa Cruz Biotechnology). Immunofluorescence of cultured cells and single fibers was performed using the following antibodies: troponin (Sigma; 1:200) and MyHC (Sigma; 1:350). Frozen muscle sections were prepared and stained as previously described. Immunofluorescence on frozen muscle sections was performed using the following antibodies: Pax 7 (Developmental Studies Hybridoma Bank; 1:100), MyoD (Santa Cruz Biotechnology; 1:100), myogenin (Santa Cruz Biotechnology; 1:200) and eMyHC (Novocastra, Leica Microsystems, 1:200). For quantification, counts were performed from a minimum of 20 randomly chosen fields, from 5-6 sections throughout the length of the muscle in 4-6 per group. All fluorescent images were captured with a Zeiss microscope (Zeiss, German).

Animal studies

Mice (C57B/L6) were housed in the animal facilities of The Chinese University of Hong Kong (CUHK) under conventional conditions with constant temperature and humidity and fed a standard diet. Animal experimentation was approved by the CUHK Animal Ethics Committee. For CTX (Latoxan, Valence, France) injection, ~7-week-old mice were injected with 50 µl of CTX (10 µM) into the tibialis anterior (TA) muscles. Oligos were prepared by preincubating 15 µm siRNA oligos with Lipofectamine 2000 for 15 min and injections were made in a final volume of 60 µl in OPTI-MEM (Invitrogen, NY, USA) on days 1/4, 2 and 4. Mice were sacrificed and TA muscles were harvested on days 0, 2, 3 and 6, and total RNAs and proteins were extracted for real-time RT-PCR and western blotting analyses. For immunofluorescene staining of MyoD, myogenin and Pax7, muscle sections were collected on day 3 and day 6 for eMyHC. Five mice were used in each group.

Acknowledgments

We thank Dr Xiaoxing Li for helping bisulfate genomic specific sequencing study. We thank Dr Prasanth KV and Qinyu Hao for their kind help and discussion on FISH experiment. The work described in this paper was substantially supported by General Research Funds (GRF) from the Research Grants Council (RGC) of the Hong Kong Special Administrative Region, China (476310 and 476113 to HW and 473713 to HS), the 973 program of Ministry of Science and Technology of China (2014CB964700 and 2011CB965201), and the Strategic Priority Research Program of the Chinese Academy of Sciences (XDA01020106).

References

1 Fatica A, Bozzoni I. Long non-coding RNAs: new players in cell differentiation and development. *Nat Rev Genet* 2014; **15**:7-21.
2 Brockdorff N. Noncoding RNA and Polycomb recruitment. *RNA* 2013; **19**:429-442.
3 Mercer TR, Mattick JS. Structure and function of long noncoding RNAs in epigenetic regulation. *Nat Struct Mol Biol* 2013; **20**:300-307.
4 Ulitsky I, Bartel DP. lincRNAs: genomics, evolution, and mechanisms. *Cell* 2013; **154**:26-46.
5 Buckingham M. Myogenic progenitor cells and skeletal myogenesis in vertebrates. *Curr Opin Genet Dev* 2006; **16**:525-532.
6 Saccone V, Puri PL. Epigenetic regulation of skeletal myogenesis. *Organogenesis* 2010; **6**:48-53.
7 Lucarelli M, Fuso A, Strom R, Scarpa S. The dynamics of myogenin site-specific demethylation is strongly correlated with its expression and with muscle differentiation. *J Biol Chem* 2001; **276**:7500-7506.
8 Mohammad F, Mondal T, Guseva N, Pandey GK, Kanduri C. Kcnq1ot1 noncoding RNA mediates transcriptional gene silencing by interacting with Dnmt1. *Development* 2010; **137**:2493-2499.
9 Di Ruscio A, Ebralidze AK, Benoukraf T, *et al.* DNMT1-interacting RNAs block gene-specific DNA methylation. *Nature* 2013; **503**:371-376.

10 Sun K, Zhao Y, Wang H, Sun H. Sebnif: an integrated bioinformatics pipeline for the identification of novel large intergenic noncoding RNAs (lincRNAs) — application in human skeletal muscle cells. *PLoS One* 2014; **9**:e84500.
11 Guttman M, Amit I, Garber M, *et al.* Chromatin signature reveals over a thousand highly conserved large non-coding RNAs in mammals. *Nature* 2009; **458**:223-227.
12 Du J, Chen T, Zou X, Xiong B, Lu G. Dppa2 knockdown-induced differentiation and repressed proliferation of mouse embryonic stem cells. *J Biochem* 2010; **147**:265-271.
13 Lu L, Sun K, Chen X, *et al.* Genome-wide survey by ChIP-seq reveals YY1 regulation of lincRNAs in skeletal myogenesis. *EMBO J* 2013; **32**:2575-2588.
14 Sun K, Chen X, Jiang P, Song X, Wang H, Sun H. iSeeRNA: identification of long intergenic non-coding RNA transcripts from transcriptome sequencing data. *BMC Genomics* 2013; **14** Suppl 2:S7.
15 Cao Y, Yao Z, Sarkar D, *et al.* Genome-wide MyoD binding in skeletal muscle cells: a potential for broad cellular reprogramming. *Dev Cell* 2010; **18**:662-674.
16 Lu L, Zhou L, Chen EZ, *et al.* A novel YY1-miR-1 regulatory circuit in skeletal myogenesis revealed by genome-wide prediction of YY1-miRNA network. *PLoS One* 2012; **7**:e27596.
17 Wang L, Zhou L, Jiang P, *et al.* Loss of miR-29 in myoblasts contributes to dystrophic muscle pathogenesis. *Mol Ther* 2012; **20**:1222-1233.
18 Zhou L, Wang L, Lu L, Jiang P, Sun H, Wang H. A novel target of microRNA-29, Ring1 and YY1-binding protein (Rybp), negatively regulates skeletal myogenesis. *J Biol Chem* 2012; **287**:25255-25265.
19 Zhou L, Wang L, Lu L, Jiang P, Sun H, Wang H. Inhibition of miR-29 by TGF-beta-Smad3 signaling through dual mechanisms promotes transdifferentiation of mouse myoblasts into myofibroblasts. *PLoS One* 2012; **7**:e33766.
20 Guil S, Esteller M. Cis-acting noncoding RNAs: friends and foes. *Nat Struct Mol Biol* 2012; **19**:1068-1075.
21 Lang KC, Lin IH, Teng HF, *et al.* Simultaneous overexpression of Oct4 and Nanog abrogates terminal myogenesis. *Am J Physiol Cell Physiol* 2009; **297**:C43-C54.
22 Ruau D, Ensenat-Waser R, Dinger TC, *et al.* Pluripotency associated genes are reactivated by chromatin-modifying agents in neurosphere cells. *Stem Cells* 2008; **26**:920-926.
23 Hupkes M, Jonsson MK, Scheenen WJ, *et al.* Epigenetics: DNA demethylation promotes skeletal myotube maturation. *FASEB J* 2011; **25**:3861-3872.
24 Kim G, Ni J, Kelesoglu N, Roberts R, Pradhan S. Co-operation and communication between the human maintenance and *de novo* DNA (cytosine-5) methyltransferases. *EMBO J* 2002; **21**:4183-4195.
25 Chu C, Qu K, Zhong FL, Artandi SE, Chang HY. Genomic maps of long noncoding RNA occupancy reveal principles of RNA-chromatin interactions. *Mol Cell* 2011; **44**:667-678.
26 Sanyal A, Lajoie BR, Jain G, Dekker J. The long-range interaction landscape of gene promoters. *Nature* 2012; **489**:109-113.
27 Taberlay PC, Kelly TK, Liu CC, *et al.* Polycomb-repressed genes have permissive enhancers that initiate reprogramming. *Cell* 2011; **147**:1283-1294.
28 Phillips-Cremins JE, Sauria ME, Sanyal A, *et al.* Architectural protein subclasses shape 3D organization of genomes during lineage commitment. *Cell* 2013; **153**:1281-1295.
29 Kagey MH, Newman JJ, Bilodeau S, *et al.* Mediator and cohesin connect gene expression and chromatin architecture. *Nature* 2010; **467**:430-435.
30 Zhang H, Zeitz MJ, Wang H, *et al.* Long noncoding RNA-mediated intrachromosomal interactions promote imprinting at the Kcnq1 locus. *J Cell Biol* 2014; **204**:61-75.
31 Cheung TH, Quach NL, Charville GW, *et al.* Maintenance of muscle stem-cell quiescence by microRNA-489. *Nature* 2012; **482**:524-528.
32 Wang H, Hertlein E, Bakkar N, *et al.* NF-kappaB regulation of YY1 inhibits skeletal myogenesis through transcriptional silencing of myofibrillar genes. *Mol Cell Biol* 2007; **27**:4374-4387.
33 Yang Y, Zhou L, Lu L, *et al.* A novel miR-193a-5p-YY1-APC regulatory axis in human endometrioid endometrial adenocarcinoma. *Oncogene* 2013; **32**:3432-3442.
34 Zhao Y, Yang Y, Trovik J, *et al.* A novel wnt regulatory axis in endometrioid endometrial cancer. *Cancer Res* 2014; **74**:5103-5117.
35 Xiang JF, Yin QF, Chen T, *et al.* Human colorectal cancer-specific CCAT1-L lncRNA regulates long-range chromatin interactions at the MYC locus. *Cell Res* 2014; **24**:513-531.
36 Zhou L, Wang L, Lu L, Jiang P, Sun H, Wang H. A novel target of microRNA-29, Ring1 and YY1-binding protein (Rybp), negatively regulates skeletal myogenesis. *J Biol Chem* 2012; **287**:25255-25265.
37 Yang Y, Zhou L, Lu L, *et al.* A novel miR-193a-5p-YY1-APC regulatory axis in human endometrioid endometrial adenocarcinoma. *Oncogene* 2013; **32**:3432-3442.
38 Tripathi V, Ellis JD, Shen Z, *et al.* The nuclear-retained noncoding RNA MALAT1 regulates alternative splicing by modulating SR splicing factor phosphorylation. *Mol Cell* 2010; **39**:925-938.
39 Tsai MC, Manor O, Wan Y, *et al.* Long noncoding RNA as modular scaffold of histone modification complexes. *Science* 2010; **329**:689-693.
40 Han J, Kim D, Morris KV. Promoter-associated RNA is required for RNA-directed transcriptional gene silencing in human cells. *Proc Natl Acad Sci USA* 2007; **104**:12422-12427.
41 Wang H, Garzon R, Sun H, *et al.* NF-kappaB-YY1-miR-29 regulatory circuitry in skeletal myogenesis and rhabdomyosarcoma. *Cancer Cell* 2008; **14**:369-381.
42 Guttridge DC, Albanese C, Reuther JY, Pestell RG, Baldwin AS Jr. NF-kappaB controls cell growth and differentiation through transcriptional regulation of cyclin D1. *Mol Cell Biol* 1999; **19**:5785-5799.

(**Supplementary information** is linked to the online version of the paper on the *Cell Research* website.)